# REPAIR WELDING OF INTERMEDIATE CASES OF AIRCRAFT ENGINES FROM HIGH-TEMPERATURE MAGNESIUM ALLOY ML10 WITH APPLICATION OF ELECTRODYNAMIC TREATMENT

**L.M. LOBANOV**[1], **N.A. PASHCHIN**[1], **A.V. CHERKASHIN**[1], **G.I. TKACHUK**[1], **V.V. SAVITSKY**[1], **O.L. MIKHODUJ**[1], **K.V. SHIYAN**[1], **V.K. LEVCHUK**[1], **V.V. ZHYGINAS**[2] and **A.P. LYASHCHENKO**[2]

[1]E.O. Paton Electric Welding Institute, NASU, Kiev, Ukraine

[2]SC «Plant 410 of Civil Aviation», Kiev, Ukraine

Technology was developed for repair welding of damages in aircraft engine intermediate cases from magnesium alloy ML10. The technology comprises electrodynamic treatment of welds aimed at reducing the level of residual welding stresses. It was experimentally proved that treatment practically eliminates residual stresses in the weld. At charging voltage of up to 200 V electrodynamic treatment operator can perform maximum 1100 electrodynamic impact operations per shift, and at 500 V voltage — not more than 100 operations, that fully meets the requirements of production cycle of repair welding of aircraft intermediate case.

**Keywords:** *argon-arc repair welding, electrodynamic treatment, magnesium alloy, aircraft engine cases, magnetic field intensity, pulsed current, charging voltage, capacitor capacitance, welding stresses, treatment effectiveness*

Development of modern technologies of repair of aeronautical engineering equipment is related to searching for new ways of extension of service life of metal structures from high-temperature magnesium alloys, reconditioned by repair welding. One of the causes for shortening of the service life of flying vehicles are residual welding stresses in repair welds, which adversely affect the fatigue strength, corrosion resistance and residual distortion of aircraft structural elements. This necessitates investigation of advanced methods to control the stressed state of welded joints, one of which is treatment by electric current pulses [1, 2].

Method of realization of pulsed current impact on metals is electrodynamic treatment (EDT) based on initiation of electrodynamic forces in the material, arising at passage of a current discharge in the treated material [3]. The mechanisms of EDT impact on the treated material are described in detail in [4].

One of the structural components of the aircraft, in which the damage is repaired by welding, is the aircraft engine intermediate case (AEIC). AEIC purpose is aircraft engine fastening on the aircraft wing and thermal insulation of the airframe structural components from thermal impact of an operating engine. Figure 1, *a*, shows AEIC appearance as-assembled with D-36 engine. Conditions of AEIC operation make high requirements to fatigue and static strength characteristics of the structure at high (up to 400 °C) temperatures, as well as to its dimensional stability, determining the aerodynamic and propulsion performance characteristics of D-36 engine. Proceeding from that, static and fatigue strength of AEIC repair welded joints should correspond to mechanical characteristics of base metal, and level of residual welding stresses — to minimum values. Thus, it is believed to be reasonable to assess EDT capabilities to lower the level of residual welding stresses in AEIC repair welds.

The objective of this work is development of the technology of repair welding of AEIC damage with EDT application.

AEIC is a large-sized cast structure from magnesium alloy ML10 (Figure 1, *b*) which consists of outer *1* and inner *2* cylindrical shells, connected by stiffeners — posts *4*. One of the design features of the posts is presence of inner cavities in them, through which the coolant circulates, which is designed for minimizing the thermal impact of operating engine on AEIC. Outer shell is designed for mounting AEIC on aircraft wing, and the inner shell — for fastening the aircraft engine *3*.

The most characteristic damages of AEIC (Figure 2) rectified by repair welding, are fatigue cracks, disturbing the integrity of the post in the points of their connection to outer and inner shells (Figure 2, weld 1, view *A*). Formation of fatigue cracks on the external surface of outer shell in the zone of reinforcement for cooling pipeline flange (Figure 2, weld 2, sectional view *A*–*A*) and on reinforcement for the system of AEIC fastening to the wing is less common. In terms of design the assembly of AEIC fastening to the wing is similar to that shown in sectional view *A*–*A*. The result of mentioned service defects are a partial loss of the load-carrying capacity of the structure and violation of leak-tightness of AEIC cooling cavities.

Repair of AEIC damages was performed using manual single- and multipass nonconsumable electrode arc welding (TIG) in shielding gas atmosphere (argon) in the following modes: $U_a$ = = 20 V, $v_w$ = 1.5 mm/s. Shielding gas was pure argon of grade A, recommended for welding tight joints, to which welds 1 and 2 belong (argon flow rate was 0.25–0.30 l/s). Post repair (see Figure 2, weld 1) was performed at current of 200–350 A in five passes, repair of reinforcement for the cooling main pipeline (Figure 2, weld 2) — at current of 200–250 A in two passes. Joint preparation for welding was performed by mechanical cleaning of the repair joint to the width of 15–30 mm from both sides using a steel brush (stainless steel diameter of 0.2 mm) and scraping. Time interval between mechanical cleaning and welding did not exceed 24 h. Filler rods of ML9 grade of 6 mm diameter were used, the surface of which was treated by chemical etching before welding. Preparation of crack edges was performed with the angle of opening of 50–70°, with more than 3 mm radius of opening in the root up to residual thickness of 0.3–0.5 mm. TIG welding was performed with concurrent local preheating of the welding zone, which was realized by placing specialized heaters based on tubular electric heating elements on the base metal. Heating temperature was equal to 150–200 °C. The first pass was made at minimum current with the initial and final sections of the repair weld reaching the base metal. Here smooth transition of the deposited to base metal was ensured with welding up of the crater in the mode of smooth extinction of the arc. At forced stopping of the welding process, because of filler rod replacement, overlapping of earlier deposited weld by 20–30 mm was performed. The overlapped surface was first cleaned mechanically.

Presence of residual stresses in AEIC repair welds in a number of cases requires performance of postweld heat treatment of the item in large-sized electric furnaces that is a highly energy-consuming operation. Application of heat treatment is required when repair welding of more

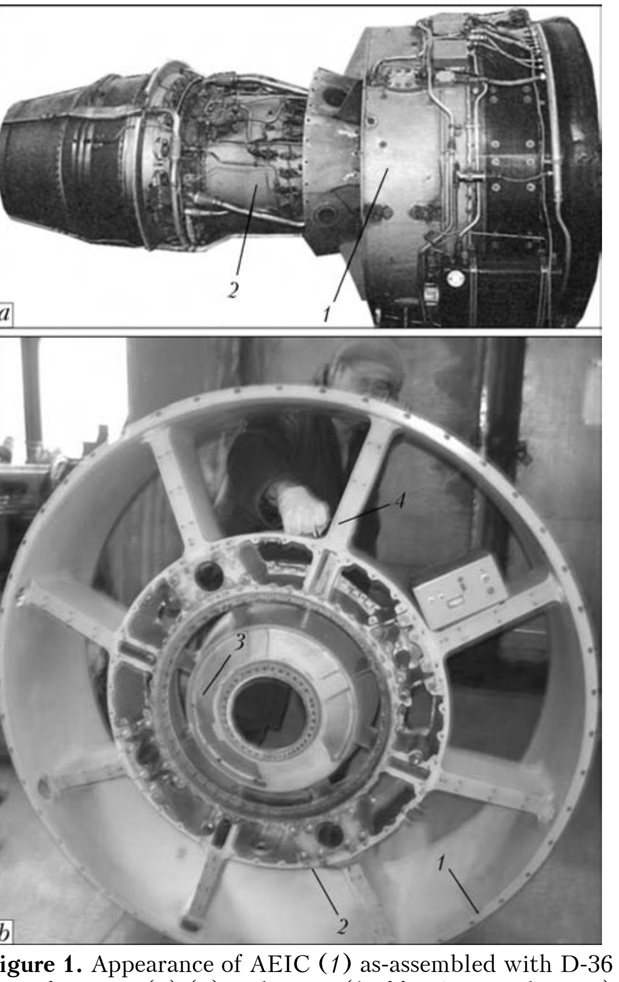


**Figure 1.** Appearance of AEIC (*1*) as-assembled with D-36 aircraft engine (*2*) (*a*) and AEIC (*b*–*f* for *1*–*4* see the text)

than two AEIC damages is performed. At the same time, there are cases, when a unit defect of small depth and length is to be repaired. Then application of total heat treatment is not rational. Practical experience of application of postweld local heating of the repair weld with tubular electric heating elements used for welding, demonstrated its low effectiveness as a result of high heat conductivity of ML10 alloy. Application of

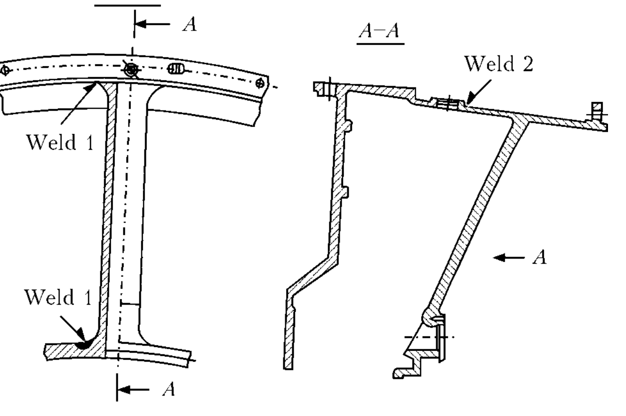


**Figure 2.** Schematic of location of repair welds at service damage of AEIC in the zone of connection of the post to the outer and inner shells (weld 1) and in the zone of fastening the cooling pipeline (weld 2)

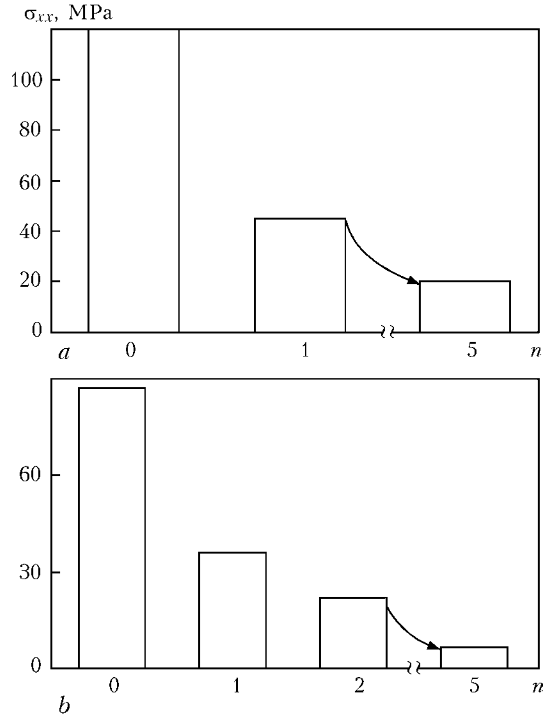


**Figure 3.** Change of values of stresses $\sigma_{xx}$ in single-pass 1 (*a*) and two-pass 2 (*b*) welds depending on the number of current discharges *n*

EDT will allow not only lowering the level of residual stresses in short repair welds without heat treatment application, but also replacing it in the future that will lower the cost of AEIC reconditioning. It should be noted that by the results of testing by static tension, EDT does not have any negative influence on mechanical characteristics of AEIC repair welded joints.

EDT influence on distribution of residual stresses arising at two-pass deposition of weld 1 was studied on samples of 350 × 200 × 8 mm size. Before bead deposition a cut of the length, width and depth of 200, 1.6–2.0 and 8–10 mm, respectively, was made with a hand cutter along the weld by a procedure described above. In order to reproduce the operations of AEIC repair, two-pass welding was performed in the cut section in the mode given above. Here, the geometrical characteristics of the deposited weld corresponded to parameters of the repair joint made in AEIC on the shop floor.

**Table 1.** Modes of EDT of welded joints of magnesium alloy ML10 (capacitor storage $C$ = 6600 μF, discharge ratio $t_r$ = 60 s)

| EDT mode number | Charging voltage $U$, V | Charging current* $I$, A | Electrode pressure* $P$, N | Discharge time* $t_d$, ms |
|---|---|---|---|---|
| 1 | 200 | 1195 | 2792 | 1.2 |
| 2 | 500 | 3080 | 20461 | 1.6 |

*Procedure of determination of EDT parameters is described in [4].

EDT influence on the magnitude and distribution of residual stresses when making weld 2 was studied on samples of 300 × 200 × 8 mm size, containing elements of reinforcement for the flange of the cooling pipeline, shown in Figure 3 (sectional view *A–A*). Before deposition a cut of the length, width and depth of 50, 1.6–2.0 and 8–10 mm, respectively, simulating the fracture, was made between the bosses, and its edge preparation was made similar to weld 1. In order to simulate repair welding performed at damage reconditioning, single-pass deposit 50 mm long was made between the bosses, in the mode mentioned above. After bead deposition and complete cooling of the samples, EDT of welded joints of the samples was performed in the modes given in Table 1.

Welded joints were treated along the weld axis in the direction from the middle towards the edges.

Before performance of TIG welding, evaluation of the initial level of stresses in ML10 alloy was performed by the method of electron speckle-interferometry on sample surface. After welding, values of longitudinal component $\sigma_{xx}$ of residual stresses were determined in repair weld zone before and after EDT performance. Treatment effectiveness was assessed by the results of comparison of stressed state parameters before and after EDT.

Evaluation of initial stressed state on the surface of ML10 alloy samples before welding showed that stress distribution on their outer surface was uniform, while $\sigma_{xx}$ values were in the range of 4–6 MPa.

EDT of samples with deposited welds 1 and 2 was performed by series of five current discharges in modes corresponding to charging voltage $U$ = 200 and 500 V. Sections on the surface of deposited beads were treated by application of current pulses with monitoring $\sigma_{xx}$ variation in EDT zone. Initial and final weld sections of 10 mm length, in which values of initial stresses are minimal, were treated in mode 1, and the other bead surfaces — in mode 2 from Table 1.

Initial $\sigma_{xx}$ values in the metal of single-pass weld 2 before and after treatment were equal to 120 and 20 MPa, respectively. Initial $\sigma_{xx}$ level in two-pass weld 1 before treatment was lower and was equal to 87 MPa. This is due to local tempering of weld metal deposited in the first pass after making the second pass. After EDT $\sigma_{xx}$ values did not exceed 6.5 MPa in the measured zone that is comparable with the stress level in the base metal before deposition. Changes of $\sigma_{xx}$ values in welds 1 and 2, depending on the number of current pulses $n$ are shown in Figure 3, from which it is seen that the maximum effectiveness of electrodynamic impact is achieved after the first current discharge ($n = 1$) that allows lowering initial $\sigma_{xx}$ values by more than 50 %.

Results of experiments conducted on AEIC fragments lead to the conclusion that EDT of repair deposits in the zone of characteristic damage of the structure allows lowering the level of initial welding stresses practically to base metal level.

EDT of full-scale AEIC was conducted in the locations of repair cladding in the areas of post damage (see Figure 1, *b*) and reinforcement for the flange of cooling pipeline fastening (Figure 4). EDT was performed in modes shown in Table 1 in the sequence corresponding to treatment of full-scale samples. During EDT cycle initial stress level was recorded before and after cladding, as well as after EDT. Analysis of current measurements of parameters of repair deposit stressed state leads to the conclusion that after EDT the level of stressed state in repair deposits is close to that of AEIC base metal.

It should be noted that manual tool for EDT (see Figure 4) enables access to AEIC repair welds in all the positions. Power source for EDT, the weight of which does not exceed 3 kg, is quite compact, that allows placing it on the surface of the treated structure in the working zone of EDT operator. EDT operators are exposed to the impact of pulsed electromagnetic fields. This is related to the fact that the tool, which is the source of magnetic radiation, is in direct contact with the operator's hand during EDT. Values of intensity $H$ of the magnetic field (MF) should not exceed limit permissible levels (LPL) specified by «State Sanitary Norms and Rules of Operation with Electromagnetic Field Sources» (DSN 3.3.6.096–2002). Determination of MF parameters, corresponding to AEIC treatment modes, is an urgent task, related to taking measures for industrial safety of EDT operators.

The main MF source is a flat inductor, which is part of the working tool [4]. Amplitude value of MF intensity at EDT operator workplace depends on pulse current, dimensions and shape of discharge circuit, as well as the distance between the performer and field source. Such MF sources as discharge circuit and capacitor storage module were not considered, in view of small values of magnetic radiation.

Proceeding from analysis of amplitude-frequency characteristics of current pulses, applied at EDT [4], conditions of MF radiation at EDT are at the lower limit of radio frequency range. This allowed isolating a frequency range from 1 up to 10 kHz, in which it is necessary to determine MF level, corresponding to electrodynamic impacts with charging voltage of 200–500 V.


**Figure 4.** AEIC EDT in the zone of repair cladding of reinforcement for the flange of fastening the post cooling pipeline: *1* — reinforcement for flange; *2* — manual tool for EDT; *3* — power source for EDT

A flat inductor was a source of MF radiation, and the operator's wrist located at the distance of 70 mm from the inductor, was selected as the zone closest to MF source.

Plate with deposited bead from ML10 alloy was used for evaluation of MP parameters.

Intensity $H$ of pulsed MF was determined using instrumentation system GFI-1 (Hall sensor), the analog signal from which was recorded by TDS-1002 oscillograph with Fourier transformation function. Certified sensor and oscillograph ensured measurement of the spectrum of MF in-

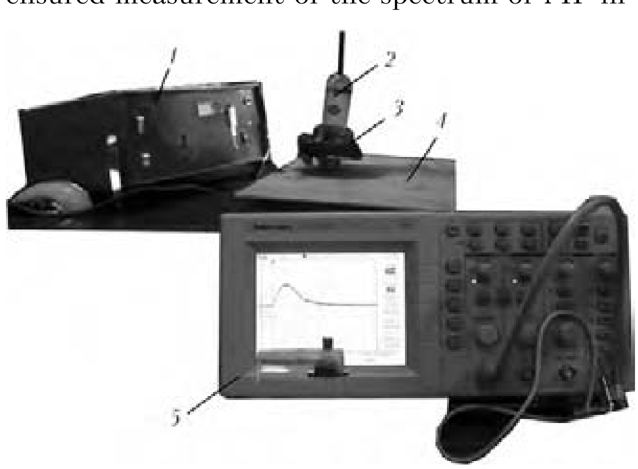


**Figure 5.** GFI-1 system for measurement of pulsed MF intensity at EDT: *1* — power source for EDT; *2* — Hall sensor; *3* — flat inductor; *4* — welded joint sample; *5* — MF intensity recorder

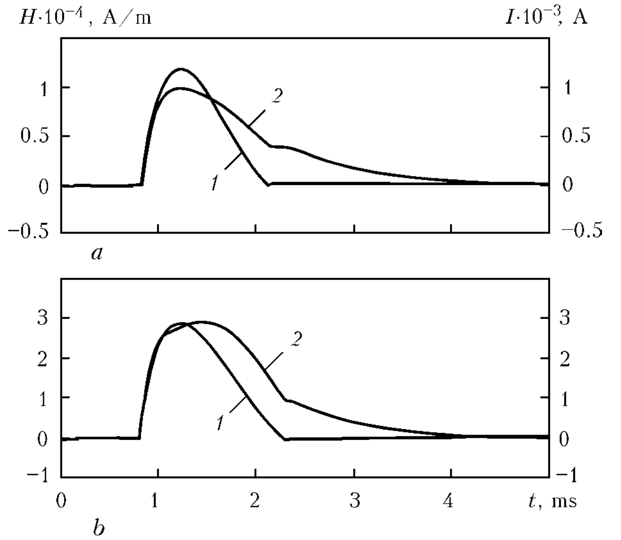


**Figure 6.** Amplitude values of pulsed current $I$ (*1*) and magnetic field intensity $H$ (*2*) at charging voltage of 200 (*a*) and 500 (*b*) V

tensity $H$ from 8 up to 16,000 A/m. Amplitude values of pulsed current were recorded using Rogowski's belt by a procedure described in [4]. Three ranges of MF frequency were studied at capacitor storage discharge, namely: 0–5, 50–1000 and 1000–10,000 Hz. Values of charging voltage of capacitor energy storage, at which MF intensity $H$ was measured, were taken to be equal to 200 and 500 V, that ensures the charge energy of 300 and 800 J, respectively, and is close to EDT parameters, used at treatment of AEIC repair welds. Hall sensor was fastened on inductor outer surface in the zone of operator hand location that allowed studying the parameters of horizontal and vertical components $H$ of magnetic flux at EDT. Recording $H$ values was conducted during an isolated discharge of capacitor storage through an inductor mounted on a welded joint sample (Figure 5).

Values of pulsed current $I$ and vertical component of intensity $H$ of pulsed MF at EDT with charging voltage of 200 and 500 V are shown in Figure 6. It should be noted that the ratio of intensity $H$ values in the vertical and horizontal planes is equal to 10/1 that allows ignoring the latter at calculation of MF characteristics.

It is found that amplitude values $I$ at $U = 200$ and 500 V are equal to 1200 and 3000 A, respectively, and the time of current running does not exceed 1.4 ms (see Figure 6, curves *1*). Amplitude $H$ values at similar $U$ values are equal to 10,000 and 30,000 A/m, respectively, and time of MF impact is equal to 2.2 ms (Figure 6, curves *2*). It should be noted that comparison of curves *1* and *2*, reflecting the ratio of values of pulsed current and MF intensity during the current discharge shows that at $I$ attenuation to zero values residual magnetic flux was recorded in the measured zone, the period of action of which is equal to 0.75–0.90 ms. At the moment of $I$ achieving zero values, intensity $H$ of residual MF at $U =$ = 200 and 500 V was equal to 4000 and 10,000 A/m, respectively. Presence of MF after current action in the discharge circuit is over, is attributable to residual magnetization of flat inductor, as well as running of attenuating current in a disc from non-ferromagnetic material, incorporated into the working tool.

**Table 2.** Spectral composition and relative energy load of MF at AEIC EDT (discharge time $t_d = 0.0022$ s)

| Charging voltage $U$, V | MF REL | | | Admissible discharge time $t_{adm}$, s | Admissible discharge number $n_{adm}$ |
|---|---|---|---|---|---|
| | Frequency range, Hz | | | | |
| | 0–5 | 50–1000 | 1000–10000 | | |
| 200 | 0.64 | 4197 | 1705 | 2.45 | 1100 |
| 500 | 8.35 | 51968 | 13426 | 0.22 | 100 |

Proceeding from the obtained data, calculation-based estimate of relative energy load (REL) in the studied spectrum of MF frequencies was performed by the following procedure [5]:

$$\mathrm{REL} = \frac{H_{\mathrm{m}}}{\mathrm{LPL}}, \quad (1)$$

where $H_m$ is the MF intensity, A/m (Hall sensor readings); LPL are the data from standard DSN 3.3.6.096–2002.

Time of operator working $t_{op}$ was assigned as an 8-hour shift, which is equal to 28,800 s. Full period of action $t_d$ of pulsed MF, as shown in Figure 6, *a*, was equal to 2.2 ms for all the studied values of charging voltage.

Admissible values of operator exposure $t_{adm}$ and number of tool switching on operations $n_{adm}$ in the studied MF were calculated by the following procedure [5]:

$$t_{\mathrm{adm}} = \frac{t_{\mathrm{op}}}{2\sum \mathrm{REL}}, \quad (2)$$

$$n_{\mathrm{adm}} = \frac{t_{\mathrm{adm}}}{t_{\mathrm{d}}}. \quad (3)$$

Data of calculation of MF parameters, given in Table 2, lead to the conclusion that at charging voltage of up to 200 V, EDT operator can perform not more than 1100 actions of thermodynamic impact per a work shift, and at 500 V voltage — not more than 100.

The number of electrodynamic impacts per one item does not exceed 20–30 discharges. Thus, production cycle of AEIC reconditioning, including EDT, provides safe working conditions for EDT operators under the condition of charging the capacitor storage up to maximum voltage value of 500 V.

**CONCLUSIONS**

1. Technology of repair welding of damage in AEIC from magnesium alloy ML10 was developed, including EDT of welds to lower the level of residual welding stresses.

2. By the results of EDT of full-scale AEIC fragments with characteristic damage of the item reconditioned by repair welding, it is established that EDT allows eliminating residual stresses in the weld.

3. Experimental procedure was developed, on the basis of which the influence of charging voltage on magnetic field intensity at EDT of welded joints of magnesium alloy ML10 was studied.

4. It is established that at up to 200 V charging voltage EDT operator can perform not more than 1100 actions of electrodynamic impact per a working shift, and at the voltage of 500 V — not more than 100, that supports the production cycle of repair welding of AEIC from magnesium alloy ML10.


1. Stepanov, G.V., Babutsky, A.I. (2007) Modeling of stress relaxation under action of pulsed electric current of high density. *Problemy Prochnosti*, **2**, 113–120.
2. Antonov, Yu.A., Ragozin, Yu.I. (2001) Pulse method of residual stress relieving. *Fizika i Khimiya Obrab. Materialov*, **3**, 91–95.
3. Lobanov, L.M., Pashchin, N.A., Loginov, V.P. et al. (2007) Change of the stress-strain state of welded joints of aluminium alloy AMg6 after electrodynamic treatment. *The Paton Welding J.*, **6**, 7–14.
4. Lobanov, L.M., Pashchin, N.A., Cherkashin, A.V. et al. (2012) Efficiency of electrodynamic treatment of aluminium alloy AMg6 and its welded joints. *Ibid.*, **1**, 2–6.
5. Levchenko, O.G. (2010) *Occupational safety and health in welding engineering*. Kiev: Osnova.


# PROCEDURE FOR CALCULATION OF DIMENSIONS OF NOZZLES IN WELDING USING TWO SEPARATE GAS JETS


**V.M. BELOKON** and **A.O. KOROTEEV**

State Institution of Higher Professional Education «Belarusian-Russian University», Mogilyov, Republic of Belarus



Advantages of the process of welding without short-circuiting with double gas shielding of the arcing zone are shown. The arc is shielded by argon, and the weld pool — by carbon dioxide gas, fed through two concentrically located nozzles. Calculation of arc radius in its largest cross-section was performed. Calculation of weld pool length allows determination of the diameter of nozzle for carbon dioxide feed. Application of higher welding parameters requires increasing the diameter of nozzles, which can be calculated by similar procedures.



***Keywords:*** *arc welding, consumable electrode, shielding gases, separate jets, dimensions of nozzles, calculation procedure*


Gas shielded welding finds wide application in production of various structures. At that $CO_2$ welding or welding in its mixtures with oxygen, argon etc. are often preferred. Welding without short-circuiting with double gas shielding, i.e. welding arc is shielded by Ar and weld metal by $CO_2$ is presented to be promising method. This method allows significantly reducing losses for electrode metal spattering, expenses for cleaning of near-weld zone from spatters and shielding gas costs [1–4].

Main parameters of each jet of shielding gas were experimentally determined by a number of domestic and foreign researchers and recommendations were provided for selection of dimensions of welding torch nozzles [5 et al.].



The aim of the present work is a development of procedure for calculation and determination of dimensions of nozzles (for Ar and $CO_2$) in reversed polarity current welding with two radial jets of shielding gases.

An electric arc consisting of three areas (anode, cathode and column) is used as a power source in consumable electrode welding. The anode and cathode areas have small dimensions. Anode spot in Ar welding can cover the whole end surface of the electrode and transfer to its side surface. At that transfer of electrode metal takes place in a form of small drops or jet that has positive effect on process of the electrode metal transfer, reducing spattering and splashing.

Argon shield of the cathode and anode areas, as well as arc column, can provide welding process, connected with positive effect of arcing in argon in welding with two concentric gas flows.

Putting of arc column to homogeneous channel with uniformly distributed within it tempera-